Li-O_2 Batteries Hot Paper

International Edition: DOI: 10.1002/anie.201600793
German Edition: DOI: 10.1002/ange.201600793

Identifying Reactive Sites and Transport Limitations of Oxygen Reactions in Aprotic Lithium-O_2 Batteries at the Stage of Sudden Death

*Jiawei Wang, Yelong Zhang, Limin Guo, Erkang Wang, and Zhangquan Peng**

Abstract: *Discharging of the aprotic Li-O_2 battery relies on the O_2 reduction reaction (ORR) forming solid Li_2O_2 in the positive electrode, which is often characterized by a sharp voltage drop (that is, sudden death) at the end of discharge, delivering a capacity far below its theoretical promise. Toward unlocking the energy capabilities of Li-O_2 batteries, it is crucial to have a fundamental understanding of the origin of sudden death in terms of reactive sites and transport limitations. Herein, a mechanistic study is presented on a model system of $Au|Li_2O_2|Li^+$ electrolyte, in which the Au electrode was passivated with a thin Li_2O_2 film by discharging to the state of sudden death. Direct conductivity measurement of the Li_2O_2 film and in situ spectroscopic study of ORR using $^{18}O_2$ for passivation and $^{16}O_2$ for further discharging provide compelling evidence that ORR (and O_2 evolution reaction as well) occurs at the buried interface of $Au|Li_2O_2$ and is limited by electron instead of Li^+ and O_2 transport.*

The aprotic lithium–air (O_2) battery has attracted significant interest because, theoretically, it can store 2–3 times more energy than today's state-of-the-art Li ion technology.[1] Discharging of the aprotic Li-O_2 battery relies on the O_2 reduction reaction (ORR) producing solid Li_2O_2 in the positive electrode, which, after a more or less constant voltage plateau, is often terminated by a sharp voltage drop (that is, sudden death), delivering a capacity far below its theoretical promise.[2,3] The charging behaviors (O_2 evolution reaction, OER), however, vary significantly and strongly depend on the discharging rate, overpotential and depth of discharge, in addition to the cell configuration (electrolyte, catalyst, and cathode material).[4] Usually, a high polarization ($\eta > 1$ V) upon charging is observed for Li-O_2 cells that have been discharged to the state of sudden death.[5]

To realize the high energy density of the aprotic Li-O_2 batteries, many research efforts have been devoted to the understanding of the limitations of Li-O_2 electrochemistry.[6–20] It is generally accepted that at the end of discharge the cathode active surface has been passivated by solid Li_2O_2,[6] a wide band-gap insulator.[7,8] A combined theoretical and experimental study by Viswanathan et al.[9] demonstrated that a thin film of Li_2O_2 (5–10 nm) can result in the discharging termination due to a limited electronic conductivity of Li_2O_2 that prevents the electron transport from the cathode surface to the reactive site that has been thought to be at the $Li_2O_2|Li^+$ electrolyte interface.[10] However, Li_2O_2 deposits in the form of particles as large as 1 μm in diameter have been frequently observed in many reports.[11,12] To account for the observation of these large particulate Li_2O_2, alternative transport mechanisms, such as transport along metal-type surfaces or hole polaron transport through bulk Li_2O_2, are proposed.[8,13–15] More recently, Aetukuri et al.[16] reported that solvating additives (such as H_2O) in aprotic electrolytes can drive solvent-mediated Li_2O_2 formation by solvating O_2^- intermediate, which is not limited by the transport properties of Li_2O_2. Johnson et al.[17] reported that aprotic solvents having high solvating capabilities (or donor numbers) can also promote the dissolution of LiO_2 and therefore the subsequent formation of Li_2O_2 in solution phase. Their findings, however, are in contrast to those of Zheng et al.,[18] who were able to build an all solid-state Li-O_2 cell in an environmental scanning electron microscopic (SEM) chamber without using any liquid electrolyte and observed the formation of large toroid particles (> 500 nm) at the end of discharge. Furthermore, they provided evidence that the growth/decomposition of Li_2O_2 is initialized on the surface of Li_2O_2 and continues along a certain direction. These findings indicate that electron and Li^+ conductivities of Li_2O_2 could support ORR and OER on Li_2O_2 surface in their system. However, Zhong et al.[19] drew a different conclusion based on an in situ transmission electron microscopy (TEM) study of the oxidation of Li_2O_2 particles anchored on multiwalled carbon nanotubes (MWCNT), in which oxidation of individual Li_2O_2 particles initiated preferentially at the MWCNT|Li_2O_2 interface, but not at the interface of $Li_2O_2|LiAlSiO_x$ (a solid electrolyte used to assemble the all solid state Li-O_2 cell for the TEM study). This observation suggests that the electrochemical oxidation of Li_2O_2 is limited by electron instead of Li^+ transport. A very recent in situ TEM work on the Li-O_2 battery containing liquid electrolyte by Kushima et al.[20] showed that the discharging reaction occurred at the interface between electrolyte and the reaction product, whereas in charging, the reactant was decomposed at the contact with the cathode, indicating that the Li^+ ion diffusivity/electronic conductivity is the limiting factor in discharging/charging, respectively. However, the above in situ SEM and TEM studies are conducted under electron beam radiation (potentially damaging Li_2O_2 and inducing defects or parasitic reactions) and high charging potentials (> 6 or even 8 V)[18,19] are applied to decompose Li_2O_2, which are

[*] Dr. J. Wang, Y. Zhang, L. Guo, Prof. E. Wang, Prof. Z. Peng
State Key Laboratory of Electroanalytical Chemistry
Changchun Institute of Applied Chemistry
Chinese Academy of Science, Changchun, Jilin, 130022 (China)
E-mail: zqpeng@ciac.ac.cn

Supporting information and the ORCID identification number(s) for the author(s) of this article can be found under: http://dx.doi.org/10.1002/anie.201600793.

very different to the situation of typical Li-O_2 cells containing liquid electrolytes.[1–3]

To have a better understanding of the limitations of Li-O_2 electrochemistry, particularly at the stage of sudden death, we conducted a combined conductivity and in situ surface enhanced Raman spectroscopic (SERS, a surface-sensitive technique that can effectively detect the species in the immediate vicinity of SERS active substrates) study on a model system of Au | Li_2O_2 | Li^+ dimethyl sulfoxide (DMSO), in which the Au electrode was pre-passivated with a Li_2O_2 film (ca. 3.8 nm) by discharging to the state of sudden death. By bringing the Au | Li_2O_2 electrode in contact with a Hg pool, direct conductivity measurement of the ultrathin Li_2O_2 film has been achieved for the first time, and the electronic (σ_{eon}) and ionic (σ_{ion}) conductivities are measured to be 2.2×10^{-13} and 3.1×10^{-12} S cm^{-1}, respectively. By conducting an in situ SERS study of ORR using $^{18}O_2$ for pre-passivation and $^{16}O_2$ for further discharging, it has been found that the antecedently deposited $Li_2{}^{18}O_2$ can be gradually displaced by the subsequently formed $Li_2{}^{16}O_2$ providing direct evidence that ORR (and OER as well) occurs at the buried interface of Au | Li_2O_2, and is limited by electron instead of Li^+ and O_2 transport.

Passivation of the Au electrode with a Li_2O_2 film has been achieved by galvanostatic discharging of the Au electrode to the state of sudden death. Here, Au electrode was used because it has been proved to be relatively inert in O_2 environment[21] and an excellent substrate for SERS.[22–24] DMSO was used as the electrolyte solvent because of its considerable stability toward the reduced O_2 species.[23–25] It has been reported that discharging current density plays a critical role in the formation of Li_2O_2, that is, solution/surface formation of Li_2O_2 can be achieved by low/high current densities.[11,12] Here, a current density of 100 μA cm^{-2}, which is high enough to ensure the surface-mediated Li_2O_2 formation,[12] was used for the deposition. Discharging of the Au electrode using two other current densities, including 10 and 300 μA cm^{-2}, has also been conducted (Supporting Information, Figures S1 and S2).

Figure 1 a showed the discharge voltage profile as a function of capacity (μAh cm^{-2}) or thickness (nm), in which an initial voltage drop from open circuit potential (OCP) at about 3.0 V to 2.4 V (kinetic barrier) followed by a stable voltage plateau at about 2.4 V and then a sharp voltage drop to 1.4 V (sudden death) has been observed. At the end of discharge, a charge density of 1.03 μAh cm^{-2} has been passed, corresponding to the deposition of a Li_2O_2 film of about 3.8 nm in thickness. The Au electrode before and after discharge has been studied by SEM (Supporting Information, Figure S3), in which essentially no change in morphology has been observed suggesting a limited thickness (or amount) of Li_2O_2 formed on Au. After passivation the Au electrode was taken out of the electrolyte and rinsed carefully with dry MeCN and vacuum dried at room temperature for 12 h. The conductivity measurement of the Li_2O_2 film was accomplished by bringing the Au | Li_2O_2 electrode in contact with a Hg pool forming an Au | Li_2O_2 | Hg sandwich structure (ionic blocking electrodes). A combination of AC impedance and DC polarization techniques has been used to obtain the

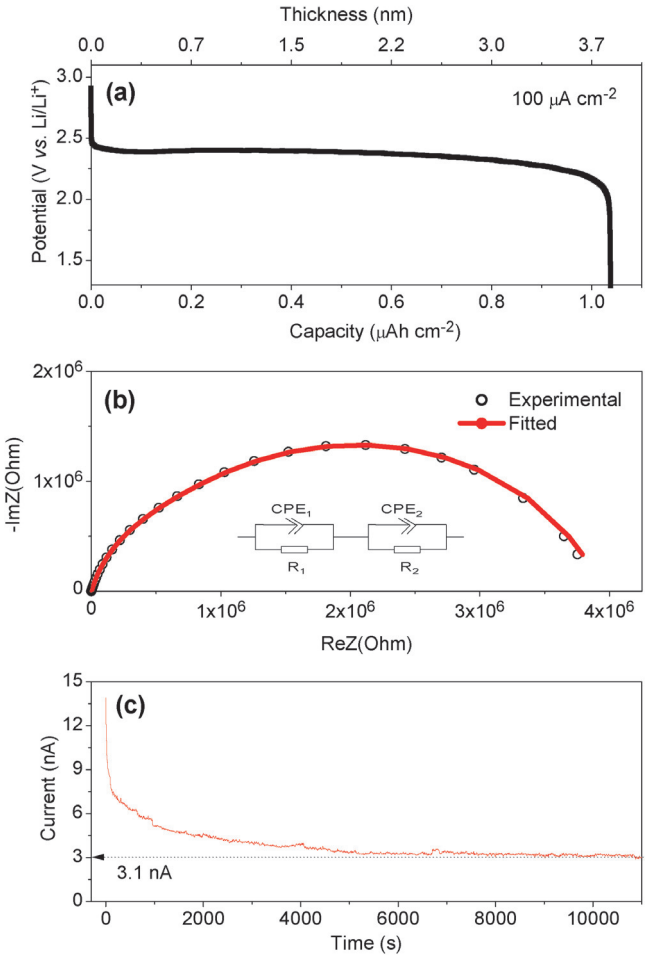

Figure 1. a) Discharging of an Au electrode to the stage of sudden death at a current density of 100 μA cm^{-2} in an O_2 saturated 0.1 M $LiClO_4$ DMSO electrolyte. b) AC impedance and c) DC polarization measurements of the obtained Li_2O_2 film. Inset in (b) shows the equivalent circuit used to fit the impedance spectrum.

conductivities according to a procedure by Gerbig et al.[8] (see also Experimental Section in the Supporting Information for details). The σ_{ion} and σ_{eon} of the Li_2O_2 film were measured to be 3.1×10^{-12} S cm^{-1} and 2.2×10^{-13} S cm^{-1}, respectively (see Figure 1 b,c; Supporting Information, Table S1), which are close to the values of nano-Li_2O_2 measured at room temperature by Dunst et al.[26] If we assume that ORR occurs at the interface of Li_2O_2 | Li^+ electrolyte, then it follows that electrons can transport from the Au to the outer surface of Li_2O_2 facing Li^+ electrolyte and the ORR is limited by Li^+ and O_2 transport. However, an σ_{eon} of 2.2×10^{-13} S cm^{-1} assisted by an overpotential of ≈1.6 V (the cutoff is 1.4 V vs. Li/Li^+) is not enough to sustain a current density of 100 μA cm^{-2} (the expected current density $=\sigma_{eon}\eta/d=$ 0.93 μA cm^{-2}). Similarly, if we presume ORR occurs at the buried interface of Au | Li_2O_2, then the limiting factor is the electron instead of Li^+ and O_2 transport through the pre-deposited Li_2O_2. However, an σ_{ion} of 3.1×10^{-12} S cm^{-1} is still too low to sustain a current density of 100 μA cm^{-2} (the expected current density $=\sigma_{ion}\eta/d=12.3$ μA cm^{-2}), and moreover, whether O_2 can transport through the Li_2O_2 film is yet

uncertain. It shall be noted that the Li_2O_2 film subjected to the conductivity measurement was in a "dry" state, which may have very different electrical properties to the "wet" Li_2O_2, provided that the Li_2O_2 film contains certain defects that can facilitate the transport of Li^+ and O_2. The discrepancy between the discharging experiment that a current density of 100 μA cm^{-2} can be sustained on Au electrode coated with a 3.8 nm Li_2O_2 film assisted by an overpotential of 1.6 V in the presence of Li^+ electrolyte, and the conductivity measurement that neither σ_{ion} nor σ_{eon} can support the charge transport through the same Li_2O_2 film in the "dry" form suggests that there must exist alternative mechanisms to maintain the ORR at the stage of sudden death.

One possibility is that the Li_2O_2 film contains certain defects through which Li^+ and O_2 can transport to reach the interface of Au | Li_2O_2. To verify this hypothesis, an in situ SERS study of ORR on Au using $^{18}O_2$ for pre-passivation and $^{16}O_2$ for further discharging was conducted. Before pre-passivation, a SERS spectrum was collected at OCP of about 3.0 V vs. Li/Li$^+$, in which only the Raman bands associated with electrolytes have been observed (Figure 2a, black curve). Then the Au electrode was discharged under $^{18}O_2$ at a current density of 100 μA cm^{-2} to the state of sudden death, and the discharge curve was essentially identical to that shown in Figure 1a. The SERS spectrum collected at the end of discharge showed a new band at about 745 cm^{-1} (^{18}O–O^{18}),[27] confirming the formation of $Li_2{}^{18}O_2$ (Figure 2a, red curve). Replacing $^{18}O_2$ with $^{16}O_2$ was realized by 10 minute purging $^{16}O_2$ through the Raman cell, during which the Au electrode potential was set to be 2.4 V. At the end of gas exchange, in situ SERS showed that $Li_2{}^{18}O_2$ still dominates on Au as expected (Figure 2a, green curve). Further discharging under $^{16}O_2$ was conducted by polarizing Au electrode at 2.0 V, a typical cathodic cutoff potential for the discharging of aprotic Li-O_2 batteries. Figure 2b showed the current–capacity (or thickness) curve of the further discharging. After 1 h discharging at 2.0 V, a weak band at about 790 cm^{-1} ascribed to the formation of $Li_2{}^{16}O_2$ was observed (Figure 2a, blue curve).[22–25] The intensity of the $Li_2{}^{16}O_2$ band increases as a function of discharging time, and one prominent feature is that prolonged discharging time (for example, > 5 h) leads to the complete disappearance of the antecedently formed $Li_2{}^{18}O_2$ and only $Li_2{}^{16}O_2$ remains, indicating that the former has been replaced by the latter. The displacement of $Li_2{}^{18}O_2$ by $Li_2{}^{16}O_2$ detected by surface-sensitive SERS technique suggests that the reactive sites of ORR are at the Au | Li_2O_2 interface, which in return provides evidence that at the stage of sudden death ORR is limited by the electron transport instead of Li^+ and O_2 transport. The SERS results also indicate that the antecedently deposited Li_2O_2 film, although apparently passivating, contains certain defects, through which the Li^+ and O_2 in electrolyte can find their way to approach the underlying Au cathode, albeit in a very slow manner. Here we did not exclude the possibility of Li_2O_2 growth via polaron transport/tunneling, particularly at the early stage of discharge;[28,29] however, we think its contribution was minor at the stage of sudden death.

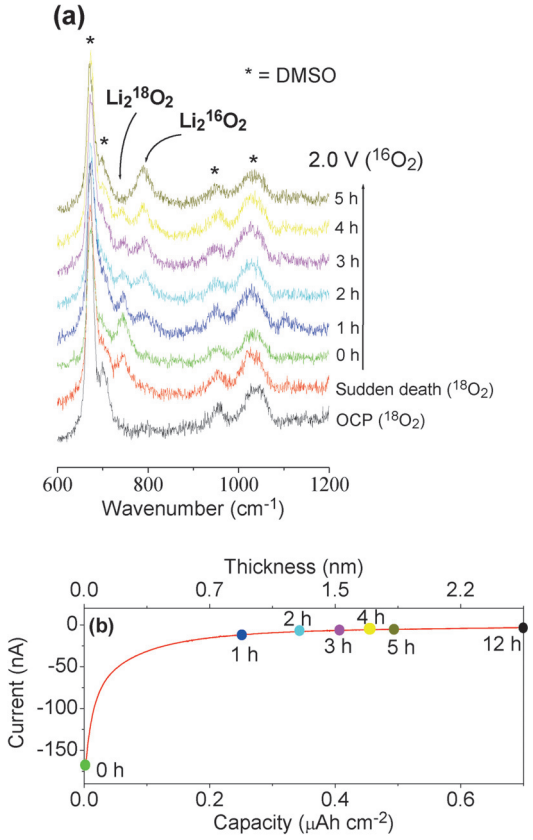

Figure 2. a) In situ SERS spectra collected at OCP (black) and at end of passivation under $^{18}O_2$ (red) followed by other spectra at various times (0–5 h) of further discharging under $^{16}O_2$ at 2.0 V vs. Li/Li$^+$. b) The current–capacity (thickness) results of the further discharging under $^{16}O_2$.

As noted above, in situ SERS showed that ORR occurs at the buried interface of Au | Li_2O_2 at the end of discharge. Subsequent recharging involves the oxidation of Li_2O_2 and therefore it would be interesting to know whether the reactive sites of OER are located at the interface of Au | Li_2O_2 or Li_2O_2 | Li^+ electrolyte. To probe OER, we deposited a mixture of $Li_2{}^{18}O_2$ and $Li_2{}^{16}O_2$ on Au by discharging to the state of sudden death under $^{18}O_2$ (see Figure 1a) followed with a further discharging under $^{16}O_2$ at constant potential of 2.0 V for 1 h (see Figure 2b). The formation of a mixed film of $Li_2{}^{18}O_2$ and $Li_2{}^{16}O_2$ has been confirmed by in situ SERS (Figure 3a, red curve), and in this case $Li_2{}^{18}O_2$ on Au has been partially displaced by subsequently formed $Li_2{}^{16}O_2$ so that both $Li_2{}^{18}O_2$ and $Li_2{}^{16}O_2$ can be detected by SERS effectively. Electrochemical oxidation of the mixed film was conducted by a linear potential scan (2 mV s^{-1}) from OCP (ca. 2.8 V) to 4.0 V (Figure 3b), and the corresponding charge and amount of Li_2O_2 (transformed into thickness) were also plotted as a function of potential (Supporting Information, Figure S4). Before the onset potential of oxidation (ca. 3.0 V), two bands at 745 and 790 cm^{-1} were observed, indicating the coexistence of antecedently deposited $Li_2{}^{18}O_2$ and subsequently formed $Li_2{}^{16}O_2$. Following potential scan showed that the subsequently formed $Li_2{}^{16}O_2$ is the species that is earlier to decompose than pre-deposited $Li_2{}^{18}O_2$ because when the 790 cm^{-1} band disappears the 745 cm^{-1} one still remains. It is interesting to note that two oxidation peaks and one oxidation

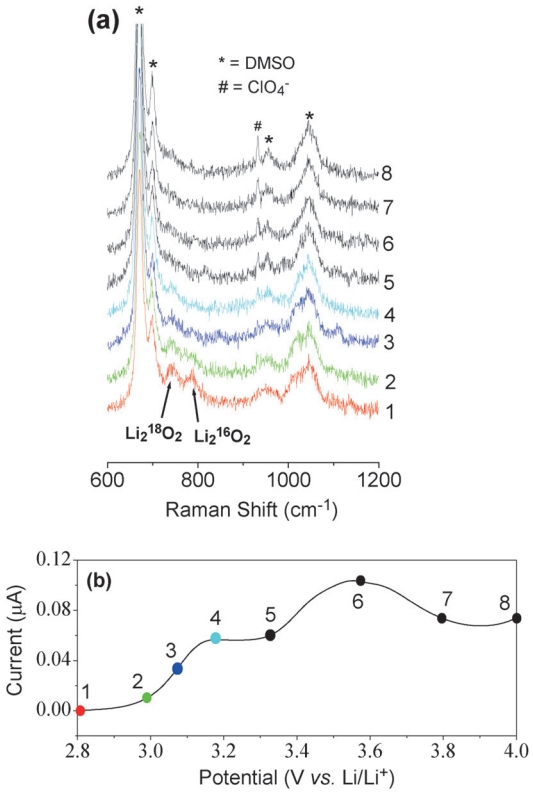

Figure 3. a) In situ SERS spectra collected during a linear potential scan from 2.8 to 4.0 V vs. Li/Li^+ on an Au electrode passivated by a mixed film of $Li_2{}^{18}O_2$ and $Li_2{}^{16}O_2$. b) The current–potential curve of the linear potential scan. Scan rate is 2 mVs^{-1}.

tail were observed for the Li_2O_2 oxidation process. We assign the peak at about 3.15 V to the oxidation of Li_2O_2 immediately adjacent to Au electrode, and the peak at about 3.55 V and the tail higher than 3.8 V to the oxidation of Li_2O_2 away from the Au surface. At the end of the first oxidation peak a circa 0.6 nm Li_2O_2 layer has been removed (Supporting Information, Figure S4), and the corresponding SERS spectra showed the disappearance of both the $Li_2{}^{18}O_2$ and $Li_2{}^{16}O_2$. At this moment a gap was formed between the Au and the remaining Li_2O_2, and the electrolyte could fill in the gap because the signal of ClO_4^- ions (931 cm^{-1}) was significantly enhanced, indicating their adsorption on Au. The remaining Li_2O_2 that is not in direct contact with Au needs a higher voltage to decompose and is out of the detection range of SERS and therefore loses its Raman signal.[30] At the end of the second oxidation peak at about 3.8 V (Supporting Information, Figure S4), a 1.8 nm Li_2O_2 layer has been removed, and at the end of potential scan to 4.0 V, 2.2 nm Li_2O_2 in total has been decomposed, which is still far below the deposited $Li_2{}^{18}O_2$ (3.8 nm, refer to Figure 1 a) and $Li_2{}^{16}O_2$ (0.8 nm, see Figure 2 b). The above in situ SERS results indicated that the oxidation of the Li_2O_2 film initializes at the interface of Au | Li_2O_2 and is limited by the electron transport. Furthermore, those parts of the Li_2O_2 away from the cathode surface, which cannot be efficiently oxidized even at high voltages (> 4.0 V), highlights the importance of using soluble molecular catalysts (that is, redox mediators) to improve OER efficiency.[31]

In conclusion, by carrying out direct conductivity measurement of a Li_2O_2 film formed by discharging to the state of sudden death, and by performing an in situ SERS study on ORR using $^{18}O_2$ for passivation and $^{16}O_2$ for further discharging, we provide evidence that at the end of discharge, ORR (and OER as well) occurs at the buried interface of Au | Li_2O_2 and is limited by electron instead of Li^+ and O_2 transport. These new findings and improved understandings of the O_2 electrochemistry at the stage of sudden death of Li-O_2 batteries suggest that morphology control of the discharge phase of Li_2O_2 (preferably porous and amorphous) and employing soluble redox mediators will be promising strategies to improve the electrochemical performances of the aprotic Li-O_2 batteries.

Acknowledgements

Z.P. is indebted to the National Foundation of China (Grant No. 21575135 and 91545129), "Strategic Priority Research Program" of the CAS (Grant No. XDA09010401), the Science and Technology Development Program of the Jilin Province (Grant No. 20150623002TC and 20160414034GH) and the "Recruitment Program of Global Youth Experts" of China.

Keywords: aprotic Li-O_2 batteries · oxygen electrochemistry · reactive sites · surface enhanced Raman spectroscopy · transport limitation

How to cite: *Angew. Chem. Int. Ed.* **2016**, *55*, 5201–5205
Angew. Chem. **2016**, *128*, 5287–5291

[1] P. G. Bruce, S. A. Freunberger, L. J. Hardwick, J.-M. Tarascon, *Nat. Mater.* **2012**, *11*, 19–29.
[2] J. Lu, L. Li, J.-B. Park, Y.-K. Sun, F. Wu, K. Amine, *Chem. Rev.* **2014**, *114*, 5611–5640.
[3] A. C. Luntz, B. D. McCloskey, *Chem. Rev.* **2014**, *114*, 11721–11750.
[4] P. Adelhelm, P. Hartmann, C. L. Bender, M. Busche, C. Eufinger, J. Janek, *Beilstein J. Nanotechnol.* **2015**, *6*, 1016–1055.
[5] X. Guo, N. Zhao, *Adv. Energy Mater.* **2013**, *3*, 1413–1416.
[6] S. Lau, L. A. Archer, *Nano Lett.* **2015**, *15*, 5995–6002.
[7] F. Tian, M. D. Radin, D. J. Siegel, *Chem. Mater.* **2014**, *26*, 2952–2959.
[8] O. Gerbig, R. Merkle, J. Maier, *Adv. Mater.* **2013**, *25*, 3129–3133.
[9] V. Viswanathan, K. S. Thygesen, J. S. Hummelshøj, J. K. Nørskov, G. Girishkumar, B. D. McCloskey, A. C. Luntz, *J. Chem. Phys.* **2011**, *135*, 214704.
[10] P. Albertus, G. Girishkumar, B. McCloskey, R. S. Sánchez-Carrera, B. Kozinsky, J. Christensen, A. C. Luntz, *J. Electrochem. Soc.* **2011**, *158*, A343–A351.
[11] R. R. Mitchell, B. M. Gallant, C. V. Thompson, Y. Shao-Horn, *Energy Environ. Sci.* **2011**, *4*, 2952–2958.
[12] B. D. Adams, C. Radtke, R. Black, M. L. Trudeau, K. Zaghib, L. F. Nazar, *Energy Environ. Sci.* **2013**, *6*, 1772–1778.
[13] M. D. Radin, D. J. Siegel, *Energy Environ. Sci.* **2013**, *6*, 2370–2379.
[14] M. D. Radin, J. F. Rodriguez, F. Tian, D. J. Siegel, *J. Am. Chem. Soc.* **2012**, *134*, 1093–1103.
[15] J. M. Garcia-Lastra, J. S. G. Myrdal, R. Christensen, K. S. Thygesen, T. Vegge, *J. Phys. Chem. C* **2013**, *117*, 5568–5577.
[16] N. B. Aetukuri, B. D. McCloskey, J. M. García, L. E. Krupp, V. Viswanathan, A. C. Luntz, *Nat. Chem.* **2015**, *7*, 50–56.

[17] L. Johnson, C. Li, Z. Liu, Y. Chen, S. A. Freunberger, P. C. Ashok, B. B. Praveen, K. Dholakia, J.-M. Tarascon, P. G. Bruce, *Nat. Chem.* **2014**, *6*, 1091 – 1099.
[18] H. Zheng, D. D. Xiao, X. Li, Y. Liu, Y. Wu, J. Wang, K. Jiang, C. Chen, L. Gu, X. Wei, Y. Hu, Q. Chen, H. Li, *Nano Lett.* **2014**, *14*, 4245 – 4249.
[19] L. Zhong, R. R. Mitchell, Y. Liu, B. M. Gallant, C. V. Thompson, J. Y. Huang, S. X. Mao, Y. Shao-Horn, *Nano Lett.* **2013**, *13*, 2209 – 2214.
[20] A. Kushima, T. Koido, Y. Fujiwara, N. Kuriyama, N. Kusumi, J. Li, *Nano Lett.* **2015**, *15*, 8260 – 8265.
[21] E. Yeager, *Electrochim. Acta* **1984**, *29*, 1527 – 1537.
[22] Z. Peng, S. A. Freunberger, L. J. Hardwick, Y. Chen, V. Giordani, F. Bardé, P. Novák, D. Graham, J.-M. Tarascon, P. G. Bruce, *Angew. Chem. Int. Ed.* **2011**, *50*, 6351 – 6355; *Angew. Chem.* **2011**, *123*, 6475 – 6479.
[23] Z. Peng, S. A. Freunberger, Y. Chen, P. G. Bruce, *Science* **2012**, *337*, 563 – 566.
[24] Z. Peng, Y. Chen, P. G. Bruce, Y. Xu, *Angew. Chem. Int. Ed.* **2015**, *54*, 8165 – 8168; *Angew. Chem.* **2015**, *127*, 8283 – 8286.
[25] Q. Yu, S. Ye, *J. Phys. Chem. C* **2015**, *119*, 12236 – 12250.
[26] A. Dunst, V. Epp, I. Hanzu, S. A. Freunberger, M. Wilkening, *Energy Environ. Sci.* **2014**, *7*, 2739 – 2752.
[27] G. Mestl, M. P. Rosynek, J. H. Lunsford, *J. Phys. Chem. B* **1998**, *102*, 154 – 161.
[28] J. Højberg, B. D. McCloskey, J. Hjelm, T. Vegge, K. Johansen, P. Norby, A. C. Luntz, *ACS Appl. Mater. Interfaces* **2015**, *7*, 4039 – 4047.
[29] K. B. Knudsen, A. C. Luntz, S. H. Jensen, T. Vegge, J. Hjelm, *J. Phys. Chem. C* **2015**, *119*, 28292 – 28299.
[30] Z. Q. Tian, X. M. Zhang in *Developments in Electrochemistry: Science Inspired by Martin Fleischmann* (Eds.: D. Pletcher, Z. Q. Tian, D. Williams), Wiley, Chichester, **2014**, pp. 113 – 135.
[31] Y. Chen, S. A. Freunberger, Z. Peng, O. Fontaine, P. G. Bruce, *Nat. Chem.* **2013**, *5*, 489 – 494.

Received: January 23, 2016
Published online: March 11, 2016

